Materials performance considerations in hydrothermal liquefaction conversion of biomass

ELLIOTT ASARE, YIMIN ZENG, AND JOSEPH KISH

ABSTRACT: Hydrothermal liquefaction (HTL) is a promising thermochemical route developed to convert woody biomass and biowaste to biochemicals and bio-oils. However, the operating conditions are rather harsh to biorefinery structural metallic components. These conditions include alkaline catalysts such as potassium carbonate (K_2CO_3); hot, pressurized (sub-critical) water reaction; and medium and aggressive anions chlorine (Cl^-) and hydrogen sulfide (H^-) released from biomass feedstocks. Thus, selection of suitable structural alloys for biorefinery components involves striking a balance between mechanical properties, corrosion resistance, and cost. Alloys currently being considered for this application include ferritic-martensitic steels and austenitic stainless steels. From a corrosion perspective in hot pressurized water, the former typically exhibits higher stress corrosion cracking resistance, whereas the latter exhibits higher corrosion resistance.

This study reviews cost-effective corrosion control strategies aimed at increasing the chromium (Cr) content for protective surface oxide formation, as screened by testing in simulated HTL alkaline water, to support materials selection and design. Corrosion control strategies include surface modification (increasing surface Cr content), alloying (increasing bulk Cr content), and stainless-steel type (ferritic vs. austenitic). Of the alloys considered (including those subjected to surface modification), ferritic stainless steels exhibit a promising balance between corrosion and stress corrosion cracking resistance, adding another family of candidate alloys for structural biorefinery component materials selection and design.

Application: The HTL conversion of woody biomass into biochemicals and bio-oils involves harsh operating conditions that are corrosive towards low-cost structural alloys. This article reviews cost-effective corrosion control strategies aimed at increasing the Cr content for protective surface oxide formation, as screened by testing in simulated HTL alkaline water. Ferritic stainless steels, as a candidate construction material for structural reactor components, exhibit a promising combination of resistance to both corrosion and stress corrosion cracking.

Hydrothermal liquefaction (HTL) is a promising cost-effective and clean thermochemical route developed for the conversion of woody biomass and biowaste to bio-oil [1-3]. The process involves contacting woody biomass with hot (250°C–374°C), pressurized (4–25 MPa) water with the addition of a catalyst (homogeneous alkaline catalyst in particular) [4-6]. The rather aggressive reaction medium requires corrosion resistance to be included along with mechanical properties and ease of fabrication considerations for cost-effective materials selection of biorefinery components. Alloys currently being considered as construction materials include ferritic-martensitic (F/M) steels, austenitic stainless steels, and nickel-based alloys [7-10].

Corrosion resistance in hot, pressurized water critically depends on the protectiveness of the surface oxide formed during immersion. The degree of protectiveness is strongly influenced by the structure and composition of the oxide films formed. The surface oxides formed on F/M steel and low-chromium (Cr) austenitic stainless steel during corrosion in hot, pressurized subcritical water are typically comprised of a more compact (protective) Cr-enriched inner M_3O_4 spinel oxide residing underneath a less compact (less protective) iron (Fe)-enriched M_3O_4 spinel oxide outer layer [11-13]. Here, M represents Fe, Cr, and nickel (Ni), depending on the alloy composition. The more-protective inner oxide is formed by a solid-state growth mechanism, whereas the less protective outer oxide is formed by a dissolution-precipitation mechanism. The degree of protectiveness of the inner oxide against further corrosion is strongly affected by the incorporated Cr content, with a higher incorporated Cr content yielding more protection [10,14]. For high-Cr stainless steels, such as Type 310 (Fe-25Cr-20Ni) and Alloy 33 (Fe-33Cr-32-Ni), an additional Cr-enriched M_2O_3 sublayer forms at the inner oxide/metal interface, which imparts further protection against corrosion. Increasing the Cr content available for incorporation into the inner oxide formed in hot pressurized water can be achieved in two ways. One way is by increasing the bulk Cr content in the alloy, which is likely a more expensive way [14]. Another way is by increasing the diffusion rate of Cr to the surface along deformed regions induced by applying a suitable mechanical surface treatment, which is likely a less expensive way. Mechanical abrasion (grinding) [15] and shot peening [16] have

been shown to reduce corrosion of stainless steels in hot pressurized water in this way.

Since HTL conversion is a pressurized process, stress corrosion cracking (SCC) resistance also requires consideration during materials selection and design. Fabricated structural components will inevitably contain welds and associated residual stresses. A metallurgical examination conducted on stainless steel components removed from bench-top, pilot-scale, and commercial-scale HTL conversion systems has indicated a cracking susceptibility [8]. Shot peening may improve SCC resistance by improving compressive surface stresses [17]; however, bulk deformation, manifested as cold work, degrades SCC resistance of austenitic stainless steel in hot pressurized water [18]. Due to intrinsic microstructure differences, ferritic stainless steels tend to be less prone to SCC than austenitic stainless steels in this harsh environment [19,20]. Thus, they deserve consideration during material selection and design, especially since HTL conversion temperatures are below those required for 475°F (246°C) embrittlement, which is a well-known materials performance limitation [21].

To help advance HTL commercialization, this study compares cost-effective corrosion control strategies aimed at increasing Cr incorporation into the inner layer of oxide films formed for improved protection against corrosion in simulated HTL alkaline water to support materials selection and design. Such strategies include alloying to increase the bulk Cr content, surface modification by mechanical treatments (including shot peening relative to a ground surface baseline) to enhance Cr diffusion to the surface during corrosion, and stainless-steel type (ferritic vs. austenitic). The research findings have been published separately elsewhere [22-25]. Here, the overall research results are compared and discussed in terms of corrosion resistance as determined by mass loss measurements and Cr incorporation into the protective inner oxide during corrosion, with some consideration given to SCC resistance.

MATERIALS AND METHODS

Materials

Table I lists the candidate commercial alloys under consideration. The chemical composition listed for each was taken from the associated Mill Certificate. The list includes one F/M steel (P91), a set of three austenitic stainless steels (SS304H, SS304L, and Alloy 33), and a set of four ferritic stainless steels (SS409, SS436, SS439, and SS444). The Cr content ranges from 9 wt% in P91 (F/M steel) to 33 wt% in Alloy 33 (advanced austenitic stainless steel). The high C version of SS304 (SS304H) was included to take advantage of high temperature with corrosion control surface treatments administered. Alloys were procured as sheet products provided in the mill annealed condition. No further heat treatments were applied once received. Rectangular test coupons were machined from the commercial sheets. All coupons were immersed in simulated HTL alkaline water after being mechanically ground to 600 grit surface finish using silicon carbide (SiC) abrasive papers and water as a lubricant. This served as a (mechanically-ground) baseline for comparison. A mechanical surface treatment (shot peening) was applied to low Cr alloys, including F/M P91 steel and austenitic Type 304H stainless steel. Details of the shot-peened (SP) treatment have been provided elsewhere [22,25].

Corrosion testing

Replicate sets of coupons were immersed in simulated HTL alkaline water for 240 h. The water was made alkaline by the addition of (reagent grade) 1 M potassium carbonate, K_2CO_3 aqueous (aq), as the inorganic conversion catalyst [5]. The corrosivity of the solution was increased by further addition of 800 ppm potassium chloride, KCl (aq), as an expected biomass contaminant released during conversion [26]. The solution was prepared using reagent grade chemicals and deionized water. The simulated HTL water was contained within an Alloy 625 liner that was placed inside

Alloy	C	Cr	Mn	Mo	Ni	Nb	Si	Ti	Fe
P91	0.11	8.4	0.5	0.9	0.1	0.06	0.3	N/R	Bal.
SS409	0.01	10.4	0.3	>0.1	0.1	0.02	0.4	0.2	Bal.
SS436	0.01	17.1	0.3	0.9	0.2	N/R	0.3	0.4	Bal.
SS439	0.02	17.5	0.3	0.1	0.2	N/R	0.3	0.4	Bal.
SS443	0.01	21.0	0.1	N/R	0.5	N/R	N/R	0.3	Bal.
SS304H	0.06	18.2	1.8	0.4	8.0	N/R	0.3	N/R	Bal.
SS304L	0.02	18.1	1.1	N/R	8.0	N/R	0.4	N/R	Bal.
Alloy 33	0.01	32.8	0.6	1.5	30.7	N/R	0.2	M/R	Bal.

C: carbon; Cr: chromium; Mn: manganese; Mo: molybdenum; Ni: nickel; Nb: niobium; Si: silicon;Ti: titanium; Fe: iron; Bal.: balance; N/R: not reported.

I. Alloy composition (wt%).

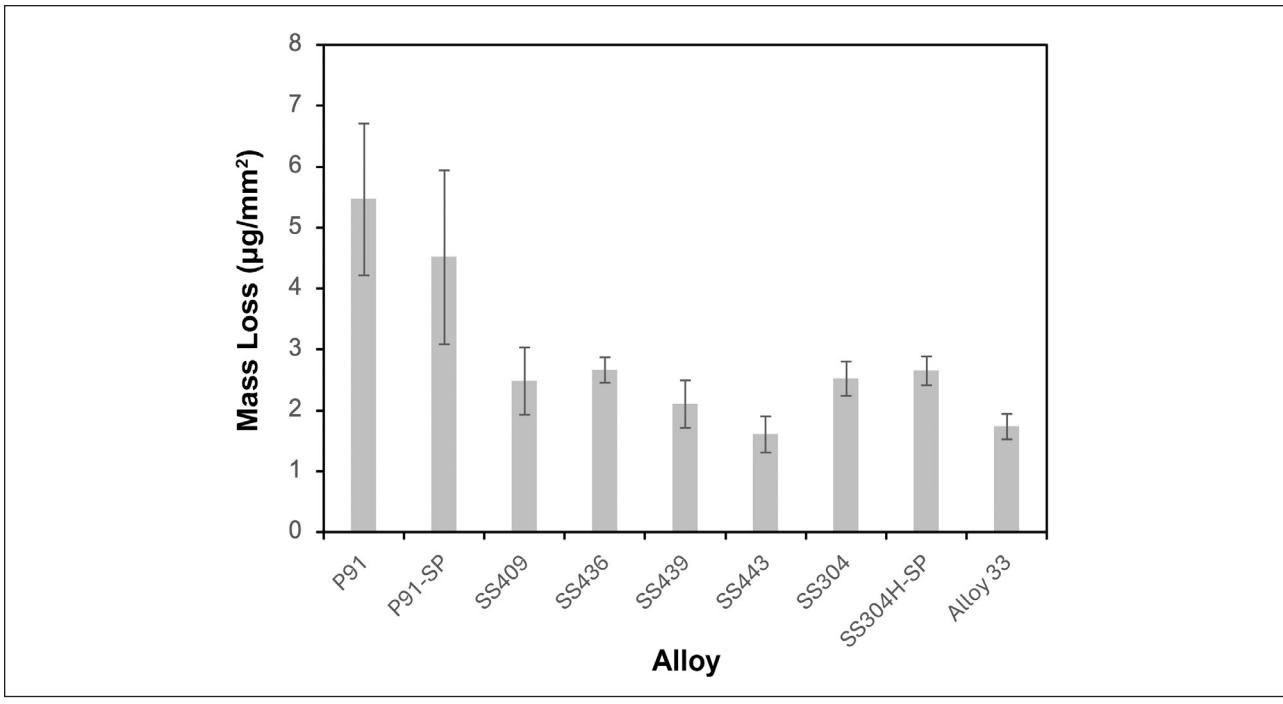

1. Mass loss (mg/mm²) exhibited by the alloys after 240 h immersion in simulated hydrothermal liquefication (HTL) water (1 M K_2CO_3 (aq) + 800 ppm KCl (aq) at 310°C and 10 MPa).

of a static Alloy C-276 autoclave. The test temperature was 310°C, and the associated saturated vapor pressure was 10 MPa. The autoclave was sealed once the replicate set of coupons were suspended, via a coupon tree, in the simulated HTL alkaline water. After sealing, the static autoclave was purged with nitrogen gas (N_2) at the beginning. After the 240-h exposure, the autoclave was cooled for 24 h prior to opening and retrieving samples. All test samples were weighed before immersion and again after chemical removal of surface corrosion products using a digital Mettler Toledo balance (Mettler Toledo; Columbus, OH, USA) with 1 µg precision. Details of the chemical removal of surface corrosion products have been provided elsewhere [24].

SCC testing

The U-bends of ferritic stainless steel SS409 and austenitic stainless steel SS304L were used to determine the relative difference in SCC susceptibility. The U-bends were prepared to the baseline mechanically-ground surface condition in the same way as the corrosion coupons prior to bending. The U-bends were made with a bending radius of 16.67 mm using a custom-built loading jig. An additional U-bend of SS304L was prepared with the SP surface treatment administered. In these SCC tests, two additional versions of the simulated HTL alkaline water were investigated: one where the 800 ppm KCl (aq) was replaced with 2,500 ppm sodium sulfide, Na_2S (aq), as an expected biomass contaminant released during conversion [26]; and another where 2,500 ppm Na_2S was added together with 800 ppm KCl (aq). Both stainless steels were tested in Solution A comprised of chlorine (Cl) and sulfur (S), whereas only SS304L was tested in Solutions B (Cl only) and C (S only) since it was the one to suffer SCC after immersion in Solution A (Cl and S). The testing time for the U-bends was 120 h.

Post-exposure characterization

Post-exposure characterization of the oxide/metal interface in cross-section was done using scanning electron microscopy (SEM) coupled with X-ray energy dispersive spectroscopy (EDS). A JEOL 6610LV scanning electron microscope (JEOL Ltd., Tokyo) equipped with an Oxford Instruments EDS system and associated AZtec software (Oxford Instruments; Abingdon, UK) was used for this purpose. The analysis (imaging and EDS elemental line scans) was done using an accelerating voltage of 15 kV and a working distance of 10 mm. Cross-section samples were prepared by cutting the samples in halves and cold mounting one half in epoxy. Cross-sectional surfaces were then mechanically abraded using SiC abrasive papers and water as a lubricant before being polished to a mirror finish using a fumed silicon dioxide (SiO_2) suspension. Depth profiling was achieved using EDS in line scan mode where the electron beam is moved across the oxide/metal interface along a line, and the X-ray data (intensity in counts per second) vs. energy in kiloelectronvolts (keV) are spot collected and subsequently analyzed for elemental compositions by the computer software.

RESULTS AND DISCUSSION

Figure 1 compares the mass loss of the alloys after immersion in the simulated HTL alkaline water for 240 h. The

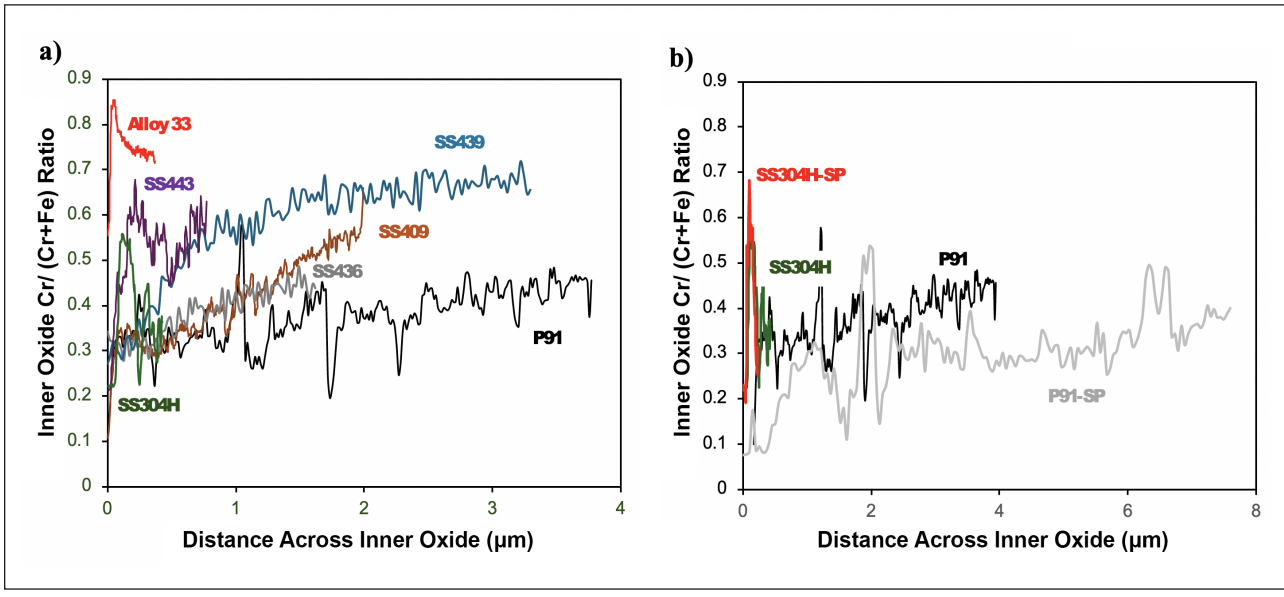

2. Chromium/chromium+iron, Cr/(Cr+Fe), ratio profile through the inner oxide formed on the alloys after 240 h immersion in simulated HTL water (1 M K_2CO_3 (aq) + 800 ppm KCl (aq) at 310°C and 10 MPa): a) with baseline mechanically-ground surface, and b) with the shot-peened (SP) surface treatment administered relative to the baseline mechanically-ground surface.

error bars represent the 95% confidence interval of the five replicate samples immersed. The set of stainless steels exhibits lower mass loss than the F/M (P91) steel. Moreover, the higher Cr-bearing stainless steels exhibit lower mass loss than lower Cr-bearing stainless steels, regardless of type (ferritic vs. austenitic). For the alloys with Cr content > 20%, further increasing Cr content does not result in a noticeable decrease in mass loss. The expectation is that, in hot pressurized water, corrosion should decrease with an increase in the bulk Cr content in the alloy [10,14]. The results reported here agree with this. Moreover, this trend holds true in the presence of aggressive chlorine (Cl^-) and hydrogen sulfide (HS^-) anions, which increase the corrosivity of HTL alkaline water [27]. The SP surface treatment administered to P91 or SS304H does not reduce the mass loss to any significant extent relative to the mechanical-ground baseline. This result does not agree with the expectation that, in hot pressurized water, corrosion should decrease with increased diffusion of Cr to the surface along deformed regions induced by shot peening the surface [16]. Analysis of the surface Cr content shows that shot peening the surface was effective in elevating the Cr content relative to the mechanically-ground baseline prior to immersion, but ineffective in maintaining that elevated content during immersion [22,25].

Figure 2a–2b compares the Cr/(Cr+Fe) concentration (at /%) ratio depth profile acquired across the protective inner oxide formed on the samples. These depth profiles were acquired using SEM-EDS, except for Alloy 33, which required scanning transmission electron microscopy (STEM) coupled with electron energy loss spectroscopy (EELS) because of the relatively small thickness of surface oxide formed [25]. In all cases, the inner oxide is an M_3O_4 spinel-type oxide [22,24,25], except for Alloy 33 where the inner oxide (actually a sublayer in the inner oxide located at the inner oxide/metal interface) is an M_2O_3 corundum-type oxide [25]. The set of stainless steels exhibits a higher Cr/(Cr+Fe) ratio in the inner oxide than the F/M steel (P91). Moreover, the higher Cr-bearing stainless steels exhibit a higher Cr/(Cr+Fe) ratio in the inner oxide than the lower Cr-bearing stainless steels, regardless of type (ferritic vs. austenitic). These results are consistent with the findings reported for austenitic stainless steels immersed in hot pressurized water where an increasing Cr/(Cr+Fe) ratio in the inner oxide coincided with an increasing bulk Cr content [14]. Shot peening the surface of P91 or SS304H does not increase the Cr/(Cr+Fe) ratio in the inner oxide layer to any sustained significant extent relative to the mechanical-ground baseline. However, there seems to be an increase in ratio for both alloys at the outer/inner oxide interface (origin of the Fig. 2b plot), which extends to a greater distance in the inner oxide on P91. Thus, the elevated surface Cr content induced by shot peening likely led to an increase in Cr/(Cr+Fe) of the inner oxide during early stages of growth (corrosion), but it was ineffective in maintaining this ratio with continued growth (corrosion).

Figure 3 shows the mass loss as a function of the average Cr/(Cr+Fe) concentration (at /%) ratio within the inner oxide for all tested alloys. The general trend shows that mass loss decreases with an increase in Cr/(Cr+Fe) ratio. The mass loss decrease is larger (steeper slope) at lower Cr/(Cr+Fe) ratios. Increasing the bulk Cr content is a more effective corrosion control strategy than administering a mechanical surface treatment (shot peening in this case). The SP surface treatment does not reduce corrosion of either P91 or SS304H to any statistically significant extent (at least

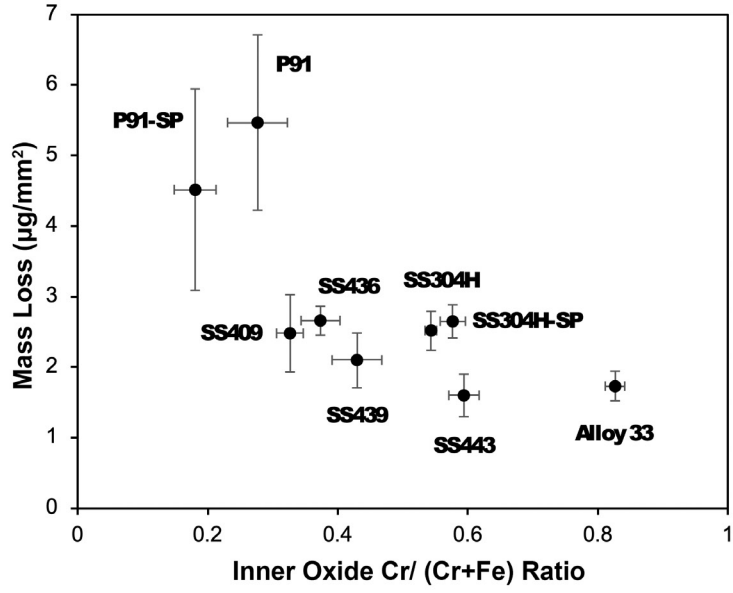

3. Mass loss (mg/mm²) as a function of the Cr/(Cr+Fe) ratio profile through the inner oxide formed on the alloys after 240 h immersion in simulated HTL water (1 M K_2CO_3 (aq) + 800 ppm KCl (aq) at 310 °C and 10 MPa).

after 240 h exposure). This indicates that increased subsurface dislocation density induced by shot peening is a secondary effect at the temperature (310°C) under study, where the existing slow diffusion kinetics cannot take advantage of increased short circuit pathways, at least at these bulk Cr contents. Figure 3 suggests that an inner (barrier) oxide Cr/(Cr+Fe) ratio of ≈0.60 is required for minimized mass loss, as exhibited by SS443 and Alloy 33.

Table II summarizes the SCC susceptibility of the stainless steel (SS409 and SS304L) U-bends immersed in simulated HTL alkaline water with aggressive anions (HS^- and Cl^-). Stress corrosion cracking was not observed for SS409 after immersions in the more aggressive Solution A (S+Cl). In contrast, SCC was observed for SS304L after immersion in this solution in both surface treated conditions (mechanically-ground baseline and shot peened). As **Fig. 4** shows, the cracking was more severe in SS304L-SP as the U-bend fractured during the 120 h immersion (Fig. 4c), whereas the SS304L U-bend did not (Fig. 4b). The metallographic examination of the cracking in cross-section (Fig. 4d and Fig. 4e) reveals that the SCC mode is largely transgranular (with some propagation along grain boundaries). In both cracking cases, preferential oxidation of deformation bands (arising from cold working) is clearly visible. These deformation bands have been identified as precursors for SCC of stainless steel in hot pressurized water relevant to nuclear power plants [28,29]. The SCC was not observed for SS304L after immersion in either solution that isolated the aggressive ions (HS^- in Solution B or Cl^- in Solution C). The results indicate that the metallurgical structure (ferrite vs. austenite) of the alloy does matter when considering SCC resistance in HTL water, at least at these bulk Cr contents. The results also indicate that sho peening is not an effective SCC control strategy. The benefits of residual compressive surface stresses are secondary, where the preferential oxidation of existing deformation bands locally overrides this benefit. Finally, the results also indicate there are at least combinatory if not synergistic effects of aggressive anions, present as biomass impurities, in promoting SCC.

Collectively, these research findings can help inform the

Solution	K_2CO_3 (aq)	KCl (aq)	Na_2S (aq)	SS409	SS304L	SS304L-SP
A (Cl and S)	1 M	800 ppm	2,500 ppm	No SCC	SCC	SCC
B (Cl only)	1 M	0 ppm	2,500 ppm	N/T	No SCC	N/T
C (S only)	1 M	800 ppm	0 ppm	N/T	No SCC	N/T

Cl: chlorine; S: silicon; K_2CO_3: potassium carbonate; aq: aqueous; KCl: potassium chloride; Na_2S: sodium sulfide; N/T: not tested.

II. U-bend stress corrosion cracking (SCC) results.

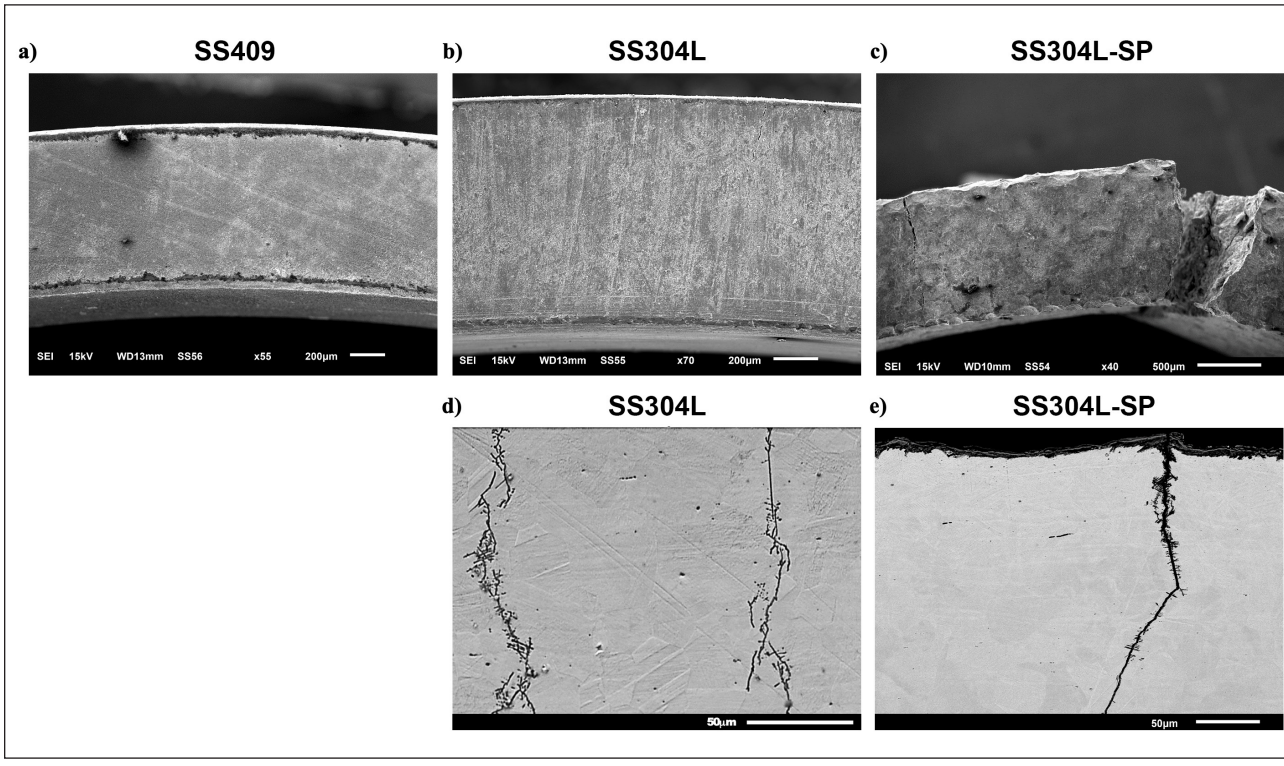

4. Secondary electron images of the stainless-steel U-bends after 120 h immersion in Solution A (Cl+S): a) SS409, b) SS304L, and c) SS304L-SP. Backscattered electron image of the cracking in cross-section: d) SS304L and e) SS304L-SP.

selection of more cost-effective, corrosion/SCC-resistant structural materials for application in HTL conversion processes. **Table III** summarizes the qualitative relative material performance of alloys based on the test results. Colors have been assigned to qualitatively classify relative materials performance as either strong (green), intermediate (yellow), or weak (red). Interestingly, only SS443 is classified as green for both corrosion and SCC resistance. All other materials are classified as yellow or red in either corrosion or SCC resistances. Following SS443, in terms of relative materials performance, are the lower Cr containing ferritic stainless steels (SS409, SS436, and SS439) — all of which are classified as yellow for corrosion resistance and green for SCC resistance. The SCC resistance of Alloy 33 should be evaluated, considering this alloy exhibited the lowest mass loss of the set of alloys considered. More realistic cases need to be considered to provide more confidence in the relative material performance observations

Alloy	Alloy Structure	Inner Oxide Structure	Inner Oxide Cr/(Cr+Fe)	Corrosion Resistance	SCC Resistance
P91	F/M	M_3O_4	0.28	R	G
P91-SP	F/M	M_3O_4	0.18	R	G
SS409	Ferritic	M_3O_4	0.33	Y	G
SS436	Ferritic	M_3O_4	0.37	Y	G
SS439	Ferritic	M_3O_4	0.43	Y	G
SS443	Ferritic	M_3O_4	0.59	G	G
SS304	Austenitic	M_3O_4	0.54	Y	R
SS304-SP	Austenitic	M_3O_4	0.58	Y	R
Alloy 33	Austenitic	M_2O_3	0.83	G	Y

Cr: chromium; Fe: iron; SCC: stress corrosion cracking; F/M: ferritic-martensitic; M_3O_4: spinel oxide; SP: shot-peened; M_2O_3: metal oxide; R: weak performance; Y: intermediate performance; G: strong performance.

III. Qualitative relative materials performance comparison.

extracted. For example, simulated HTL water should include organic components, such as formic acid, that are expected to be released during conversion.

CONCLUSIONS

The corrosion and SCC resistance of cost-effective structural alloys for HTL conversion reactor components was compared using results acquired from testing in a simulated HTL alkaline water. Corrosion control strategies considered include increasing either the bulk Cr content (likely more expensive) in the alloy or the diffusion rate of Cr to the surface along deformed regions induced by applying a suitable mechanical surface treatment (likely less expensive). The following conclusions were extracted:

1. Stainless steels, regardless of type (ferritic or austenitic), exhibit higher corrosion resistance than F/M steels in simulated HTL alkaline water. The critical factor is the amount of Cr incorporated into the protective inner oxide that forms during immersion.
2. Increasing the bulk Cr content in the steel is a more effective corrosion control strategy than administering a mechanical surface treatment, such as shot peening, to increasing fast Cr diffusion paths (dislocation density) for Cr transport to the surface during corrosion.
3. Ferritic stainless steels exhibit higher SCC resistance than austenitic stainless steels. They exhibit a promising combination of corrosion and SCC resistance. **TJ**

ACKNOWLEDGEMENTS

Funding was provided by the Natural Resources Canada's Office of Energy Research and Development (OERD) Clean Energy and Forest Innovation programs and the Natural Science and Engineering Research Council of Canada (NSERC) Discovery Grant program. Thanks to the technical staff (Shi Chao, Jennifer Collier, and Dr. Minkang Liu) at CanmetMATERIALS for autoclave testing and at the Canadian Centre for Electron Microscopy (CCEM), with instrumentation supported by Canada Foundation for Innovation, NSERC, and McMaster University, for electron microscopy support.

LITERATURE CITED

1. Zhu, Y., Biddy, M.J., Jones, S.B., et al., *Appl. Energy* 129: 384(2014). https://doi.org/10.1016/j.apenergy.2014.03.053.
2. Dimitriadis, A. and Bezergianni, S., *Renewable Sustainable Energy Rev.* 68: 113(2017). https://doi.org/10.1016/j.rser.2016.09.120.
3. Nie, Y. and Bi, X., *Biotechnol. Biofuels* 11: 23(2018). https://doi.org/10.1186/s13068-018-1019-x.
4. Karagöz, S., Bhaskar, T., Muto, A., et al., *Chem. Eng. J.* 108: 127(2005). https://doi.org/10.1016/j.cej.2005.01.007.
5. Bhaskar, T., Sera, A., Muto, A., et al., *Fuel* 87(10-11): 2236(2008). https://doi.org/10.1016/j.fuel.2007.10.018.
6. Hammerschmidt, A., Boukis, N., Hauer, E., et al., *Fuel* 90: 555(2011). https://doi.org/10.1016/j.fuel.2010.10.007.
7. Brady, M.P., Keiser, J.R., Leonard, D.N., et al., *JOM* 66: 2583(2014). https://doi.org/10.1007/s11837-014-1201-y.
8. Liu, M., Zeng, Y., and Luo, J.-L., *Energy Fuels* 36: 3134(2022). https://doi.org/10.1021/acs.energyfuels.1c04046.
9. Liu, M., Zeng, Y., and Luo, J.-L., *Corros. Sci.* 204: 110409(2022). https://doi.org/10.1016/j.corsci.2022.110409.
10. Liu, M., Zeng, Y., and Luo, J.-L., *Corros. Sci.* 218: 111148 (2023). https://doi.org/10.1016/j.corsci.2023.111148.
11. Tapping, R.L., Davidson, R.D., McAlpine, E., et al., *Corros. Sci.* 26(8): 563(1986). https://doi.org/10.1016/0010-938X(86)90024-7.
12. Robertson, J., *Corros. Sci.* 29(11-12): 1275(1989). https://doi.org/10.1016/0010-938X(89)90120-0.
13. Stellwag, B., *Corros. Sci.* 40(2-3): 337(1998). https://doi.org/10.1016/S0010-938X(97)00140-6.
14. Terachi, T., Yamada, T., Miyamoto, T., et al., *Nucl. Sci. Technol.* 45(10): 975(2008). https://doi.org/10.1080/18811248.2008.9711883.
15. Tan, L., Ren, X., Sridharan, K., et al., *Corros. Sci.* 50(7): 2040(2008). https://doi.org/10.1016/j.corsci.2008.04.008.
16. Fisher, B., Miller, B.D., Johns, E.C., et al., *Corros. Sci.* 141: 88(2018). https://doi.org/10.1016/j.corsci.2018.06.033.
17. Povich, M.J., *Corrosion* 34(5): 162(1978). https://doi.org/10.5006/0010-9312-34.5.162.
18. Arioka, K., Yamada, T., Terachi, T., et al., *Corrosion* 63(12): 1114(2007). https://doi.org/10.5006/1.3278329.
19. Andresen, P.L., Jurewicz, T.B., and Rebak, R.B., "Stress corrosion cracking resistance of ferritic chromium steels in high temperature water," *CORROSION 2012*, NACE International, Houston, 2012, Paper no. 0000118.
20. Rebak, R.B., "Resistance of ferritic steels to stress corrosion cracking in high temperature water," *ASME Pressure Vessels Piping Conf.*, ASME, New York, 2013, Paper no. 97352.
21. Nichol, T.J., Datta, A., and Aggen, G., *Metall. Trans. A* 11:573(1980). https://doi.org/10.1007/BF02670694.
22. Asare, E.K., Zeng, Y., Kish, J.R., *Can. Metall. Q.* 60(4): 306(2021). https://doi.org/10.1080/00084433.2021.2014711.
23. Asare, E.K., Zeng, Y., Persaud, S.Y., et al., *Corrosion* 80(12): 1176(2024). https://doi.org/10.5006/4642.

ABOUT THIS PAPER

Cite this article as:
Asare, E., Zeng, Y., and Kish, J., *TAPPI J.* 24(6): 281(2025). https://doi.org/10.32964/TJ24.6.281

DOI: https://doi.org/10.32964/TJ24.6.281

ISSN: 0734-1415

Publisher: TAPPI Press

About this journal

24. Asare, E.K., Kish, J.R., and Zeng, Y., *Corrosion* 81(1): 58(2025). https://doi.org/10.5006/4643.

25. Asare, E.K., Zeng, Y., and Kish, J.R., *Corrosion* 81(2): 109(2025). https://doi.org/10.5006/4274.

26. Saleh, S.B., Flensborg, J.P., Shoulaifar, T.K., et al., *Energy Fuels* 28(6): 3738(2014). https://doi.org/10.1021/ef4021262.

27. Liu, M. and Zeng, Y., *Sustainability* 15(12): 9317(2023). https://doi.org/10.3390/su15129317.

28. Lozano-Perez, S., Yamada, T., Terachi, T., et al., *Acta Mater.* 57(18): 5361(2009). https://doi.org/10.1016/j.actamat.2009.07.040.

29. Was, G.S., Farkas, D., and Robertson, I.M., *Curr. Opin. Solid State Mater. Sci.* 16(3): 134(2012). https://doi.org/10.1016/j.cossms.2012.03.003.

ABOUT THE AUTHORS

We chose this topic for study to help support materials selection for components in hydrothermal liquefaction (HTL) of biomass to meet materials performance requirements, while considering capital costs. This research complements the previous research conducted on materials performance that has underpinned construction of pilot-scale demonstrations and commercial designs by providing a corrosion and stress corrosion cracking (SCC) assessment of cost-effective stainless steels in simulated HTL alkaline water.

The most difficult aspect of the research was conducting the immersion tests in hot pressurized water, which required the use of an autoclave test system unavailable in our corrosion laboratory. We addressed this by partnering with CanmetMATERIALS who has thi^{s} research capability and the technical expertise to operate it.

We discovered that there is little published information pertaining to the corrosion and SCC susceptibility of ferritic stainless steel in HTL water. Ferritic stainless steels serve as a cost-effective alternative to advanced austenitic stainless steels as a construction material. The most interesting finding was the combined detrimental effect of H^- and Cl^- on the SCC susceptibility of Type 304 stainless steel, as cracking was only observed with both present in the solution.

Asare

Kish

Zeng

With the results here, mills can be better informed about the corrosion and SCC susceptibility of cost-effective materials from which to fabricate structural components required for the HTL conversion of woody biomas to bio-oil.

The next step in this research involves a more systematic investigation of the SCC susceptibility of the candidate alloys to determine impurity tolerance limits as a function of the applied stress level. Another step would be to investigate the corrosion susceptibility of the candidate alloys in more realistic HTL water environments, which would include conversion products in addition to impurities.

Asare is a Ph.D. candidate and Kish is a professor in the Department of Materials Science and Engineering at McMaster University in Hamilton, ON, Canada. Zeng is research scientist at CanmetMATERIALS in Hamilton, ON, Canada. Email Kish at kishjr@mcmaster.ca.